Transfer of Voltage Independence from a Rat Olfactory Channel to the *Drosophila* Ether-à-go-go K^+ Channel

Chih-Yung Tang and Diane M. Papazian

From the Department of Physiology, School of Medicine, and Molecular Biology Institute, University of California, Los Angeles, California 90095-1751

ABSTRACT The S4 segment is an important part of the voltage sensor in voltage-gated ion channels. Cyclic nucleotide-gated channels, which are members of the superfamily of voltage-gated channels, have little inherent sensitivity to voltage despite the presence of an S4 segment. We made chimeras between a voltage-independent rat olfactory channel (rolf) and the voltage-dependent ether-à-go-go K^+ channel (eag) to determine the basis of their divergent gating properties. We found that the rolf S4 segment can support a voltage-dependent mechanism of activation in eag, suggesting that rolf has a potentially functional voltage sensor that is silent during gating. In addition, we found that the S3-S4 loop of rolf increases the relative stability of the open conformation of eag, effectively converting eag into a voltage-independent channel. A single charged residue in the loop makes a significant contribution to the relative stabilization of the open state in eag. Our data suggest that cyclic nucleotide-gated channels such as rolf contain a voltage sensor which, in the physiological voltage range, is stabilized in an activated conformation that is permissive for pore opening.

KEY WORDS: cyclic nucleotide-gated channel • voltage-gated channel • voltage dependence • potassium channel • patch clamp

INTRODUCTION

In response to depolarization of the membrane, voltage-dependent ion channels undergo conformational changes that lead to opening of the ion conduction pore. This control of channel activity by the membrane potential implies that charged or dipolar groups within the channel protein serve as voltage sensors (Hodgkin and Huxley, 1952). Many voltage-dependent Na^+, Ca^{2+}, and K^+ channels contain conserved, charged amino acids in putative transmembrane segments S2, S3, and S4 which have been studied as possible voltage-sensing residues (Stuhmer et al., 1989; Liman et al., 1991; Papazian et al., 1991; Logothetis et al., 1992; Perozo et al., 1994; Papazian et al., 1995; Planells-Cases et al., 1995).

Recently, strong evidence that the S4 segment constitutes a major component of the voltage sensor in K^+ and Na^+ channels has been reported (Yang and Horn, 1995; Aggarwal and MacKinnon, 1996; Larsson et al., 1996; Mannuzu et al., 1996; Seoh et al., 1996; Yang et al., 1996). In Shaker K^+ channels, three positively charged residues in segment S4 (R365, R368, and R371) contribute significantly to the gating charge movement that accompanies activation; this charge movement corresponds to the conformational rearrangements of the voltage sensor in response to a change in the membrane potential (Aggarwal and MacKinnon, 1996; Seoh et al., 1996). In addition, it has been demonstrated that the environments of S4 residues change upon activation. In Na^+ and K^+ channels, engineered cysteine residues in the S4 segment react with sulfhydryl reagents in a voltage-dependent manner (Yang and Horn, 1995; Larsson et al., 1996; Mannuzzu et al., 1996; Yang et al., 1996). In a skeletal muscle Na^+ channel, the reactivity of two S4 residues changes from one side of the membrane to the other upon depolarization, indicating that these positions traverse the field during activation (Yang et al., 1996).

The S4 segment does not comprise the whole voltage sensor, however. In Shaker channels, a negatively charged residue in segment S2 (E293) also contributes significantly to the gating charge movement, and residue D316 in S3 may make a smaller contribution (Seoh et al., 1996). In parallel, evidence has been presented that charged residues in segments S2, S3, and S4 experience strong, presumably short-range, electrostatic interactions in the native structure of the Shaker channel (Papazian et al., 1995; Tiwari-Woodruff et al., 1997). Taken together, these results suggest that segments S2, S3, and S4 form a structural domain that functions as the voltage sensor in voltage-dependent ion channels.

Cyclic nucleotide-gated cation channels, which are involved in sensory transduction in the visual and olfactory systems, are members of the superfamily of voltage-gated ion channels (Jan and Jan, 1990, 1992). Cyclic nucleotide-gated channels and voltage-dependent K^+

Address correspondence to Diane M. Papazian, Ph.D., Department of Physiology, UCLA School of Medicine, Box 951751, Los Angeles, CA 90095-1751. Fax: 310-206-5661; E-mail: papazian@physiology.medsch.ucla.edu

channels probably derive from a common evolutionary ancestor (Jan and Jan, 1992; Strong et al., 1993). Both channel types are formed from separate subunits, each of which contains six putative transmembrane segments (S1-S6) and a loop (P) that contributes to the pore (Kaupp et al., 1989; Dhallan et al., 1990; Jan and Jan, 1990; Miller, 1991; Goulding et al., 1992). Despite demonstrated functional homology in the pore (Heginbotham et al., 1992; Goulding et al., 1993), the properties of these channels are quite different. Whereas the membrane potential controls the activity of voltage-gated K^+ channels, cyclic nucleotide-gated channels have little or no inherent voltage sensitivity (Kaupp et al., 1989; Dhallan et al., 1990; Haynes and Yau, 1990; Goulding et al., 1992). Instead, their activity is controlled allosterically by the binding of cyclic nucleotide ligands to intracellularly located domains in the channel protein (Altenhofen et al., 1991; Goulding et al., 1994; Gordon and Zagotta, 1995; Varnum et al., 1995).

Although they are voltage independent, cyclic nucleotide-gated channels contain charged amino acids in segments S2, S3, and S4 that are conserved among voltage-gated channels (Jan and Jan, 1990), including those residues in S2 and S4 that contribute to the voltage sensor in the Shaker K^+ channel (Seoh et al., 1996). Why cyclic nucleotide-gated channels are insensitive to voltage despite the presence of voltage-sensing residues is unknown.

To address this question, we made chimeras between the *Drosophila* ether-à-go-go K^+ channel (eag)[1] and a rat olfactory channel (rolf). These channels are structurally related but have quite different gating properties. Eag is a voltage-gated, K^+-selective channel that can be modulated by cAMP (Warmke et al., 1991; Brüggemann et al., 1993; Robertson et al., 1996). In contrast, rolf is a cyclic nucleotide-gated, cation-selective channel that is voltage independent (Dhallan et al., 1990). We report that the S4 segment of rolf is capable of supporting a voltage-dependent mechanism of activation when transferred into eag, which suggests that rolf contains a potentially functional voltage-sensing domain. In addition, we report that chimeras in which the S3-S4 loop of rolf has been transferred into eag are voltage independent in the physiological voltage range. Our data indicate that this region of the rolf protein dramatically increases the relative stability of the open conformation of eag. A significant part of this stabilization is due to a single charged residue in the S3-S4 loop of rolf. Our results are consistent with the idea that cyclic nucleotide-gated channels are insensitive to voltage because the voltage-sensing domain is locked in a conformation permissive for pore opening.

[1]*Abbreviations used in this paper:* eag, ether-à-go-go; rolf, rat olfactory channel; P_o, fraction of open channels.

MATERIALS AND METHODS

Molecular Biology

Eag and rolf cDNAs, kindly provided by Drs. G. Robertson (University of Wisconsin, Madison, WI) and R. Reed (Johns Hopkins University, Baltimore, MD), respectively, were subcloned into the pGEMHE vector, kindly provided by Dr. E. Liman (Massachusetts General Hospital, Boston, MA) (Dhallan et al., 1990; Warmke et al., 1991; Liman et al., 1992). Chimeras and mutations were generated by a four primer PCR strategy (Horton et al., 1989). PCR products were digested with appropriate restriction enzymes and subcloned into the wild-type eag backbone. The sequences of all engineered constructs were verified by dideoxy sequencing.

For in vitro transcription, eag constructs were linearized with NotI, whereas the rolf subclone was linearized with NheI. Run-off transcripts of RNA were prepared and injected into *Xenopus* oocytes as previously described (Timpe et al., 1988).

Electrophysiology

Eag, chimeras, and mutants were analyzed using a two-electrode voltage clamp as previously described (Timpe et al., 1988; Papazian et al., 1991). The bath solution for recording was modified Barth's saline (Timpe et al., 1988), which contained 1 mM KCl and 88 mM NaCl. Alternatively, NaCl was replaced with KCl, resulting in an 89 mM KCl bath solution, as indicated.

Rolf was analyzed in macropatches as previously described (Papazian et al., 1995). Gigaohm seals were made in normal bath solution, which contained divalent ions (Papazian et al., 1995). After excision of inside-out patches, the cytoplasmic side of the patch was perfused with divalent-free bath solution (100 mM KCl, 10 mM HEPES, 10 mM EDTA, 10 mM EGTA, pH 7.2) using a solenoid-controlled perfusion system (Weiss et al., 1992). Activation of rolf was induced by perfusing divalent-free solution containing 1 mM cGMP. The pipette solution was based on the divalent-free solution, except that 10 nM $CaCl_2$ was added to stabilize the seal without blocking rolf channels. All recordings were made at room temperature (22°C).

To study current-voltage relationships of wild-type and mutant channels over a wide range of membrane potentials, voltage ramps were applied for 500 ms from a holding potential of −10 mV (eag) or 0 mV (rolf). Ramp-evoked currents were recorded without subtraction and subsequently corrected by setting the current amplitude equal to zero at the reversal potential for K^+.

Voltage clamp protocols were applied and data were acquired using pCLAMP v.5.5.1 software and a TL-1 Labmaster Interface (Axon Instruments, Foster City, CA) with an 80386-based computer. The voltage dependence of activation was determined by analysis of isochronal tail currents. The data were fit with a simple Boltzmann distribution using SigmaPlot v.5.0 software (Jandel Scientific, San Rafael, CA) to obtain the slope factor and midpoint potential.

RESULTS

Despite Sequence Similarity, Rolf and Eag Have Divergent Gating Properties

Eag and rolf are more closely related to each other than to the four main subfamilies of voltage-gated K^+ channels, Kv1-Kv4 (Fig. 1) (Guy et al., 1991). Putative

transmembrane segments S1-S6 and the pore-forming P loop, which are characteristic of voltage-gated K^+ channels, are found in eag and rolf. Unlike members of the Kv1-Kv4 subfamilies, however, both the eag and rolf proteins contain putative cyclic nucleotide binding domains following S6 (Fig. 1 *A*) (Guy et al., 1991). The S4 segments of eag and rolf contain regularly spaced, positively charged residues, like those of other members of the superfamily. At the carboxyl-terminal end of the S4 segment, however, the sequences of eag and rolf are more similar to each other than to that of a voltage-dependent K^+ channel such as Shaker (Fig. 1 *B*).

Despite their structural similarity, rolf and eag have divergent gating properties, as previously reported by others (Fig. 1 *C*) (Dhallan et al., 1990; Brüggemann et al., 1993; Robertson et al., 1996). K^+ currents through the rolf channel, expressed as a homomultimer in *Xenopus* oocytes, can be elicited by the application of 1 mM cGMP to the cytoplasmic face of an inside-out patch of membrane. In contrast, K^+ currents through the eag channel can be evoked by depolarization of the oocyte membrane using a two-electrode voltage clamp. To investigate the mechanism that underlies the divergent gating behavior of rolf and eag, we transferred regions of rolf into eag and analyzed the voltage dependence of the resulting chimeric channels after expression in *Xenopus* oocytes.

The S4 Segment of Rolf Can Support a Voltage-dependent Mechanism of Activation

One significant difference between eag and rolf is the net charge of the S4 segment. In addition to the positively charged residues arginine (R) and lysine (K), the S4 segments of eag and rolf contain negatively charged residues, aspartate (D) and glutamate (E). Assuming that R or K contributes +1 charge, D or E contributes −1 charge, and histidine (H) contributes 0 charge, the net charge of the S4 segments of eag and rolf equals +5 and +1, respectively (Fig. 2 *A*). This raises the possibility that rolf is voltage independent because the presence of a nearly balanced number of positively and negatively charged residues restricts the movement of the S4 segment in response to changes in voltage (Goulding et al., 1992).

To test this hypothesis, we replaced portions of the S4 segment in eag with the corresponding residues from rolf. Two chimeras were made. In the S4-1 chimera, only the five most divergent amino acids were replaced, reducing the net S4 charge from +5 to +2 (Fig. 2 *A*). In the S4-2 chimera, 14 amino acids, which represent most of the S4 segment, were replaced, reducing the net S4 charge from +5 to +1, the same as in rolf (Fig. 2 *A*). Both chimeras generated functional, voltage-dependent channels after expression in *Xenopus* oocytes (Fig. 2 *B*). The open probability of the S4-1 and

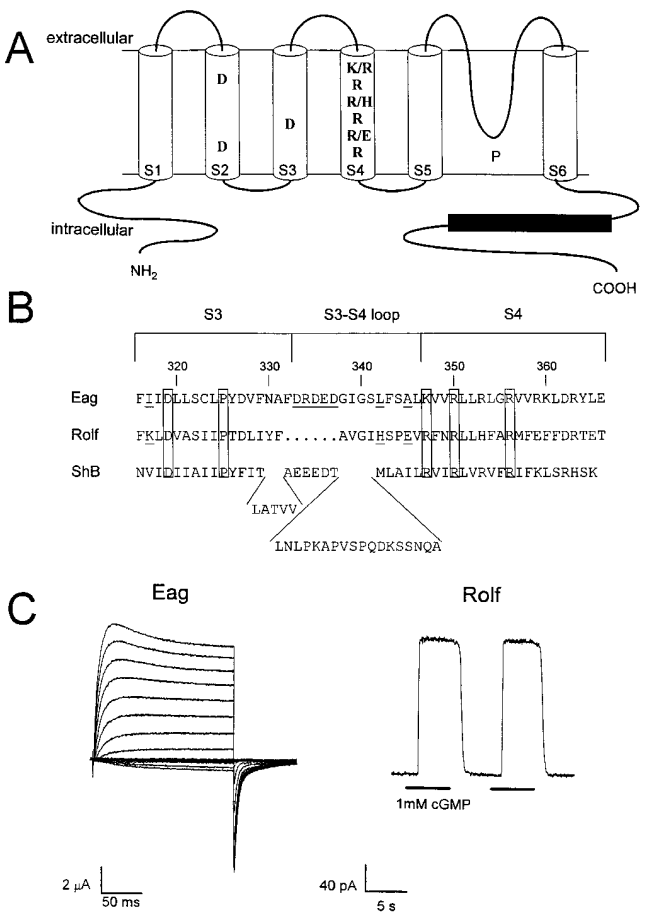

FIGURE 1. Comparison of the structural organization, sequence, and gating properties of eag and rolf. (*A*) A model for the topology of the eag and rolf subunits in the membrane. Both eag and rolf contain putative transmembrane segments S1-S6, the pore-forming P loop, and a cyclic nucleotide binding domain (*solid box*). Also shown are the approximate positions of charged residues in transmembrane segments S2, S3, and S4 that are conserved among members of the superfamily of voltage-gated channels (Jan and Jan, 1990; Chandy and Gutman, 1994). Single letters indicate the residues present in both eag and rolf. Pairs of letters indicate the residues found in eag (first) or rolf (second). (*B*) An alignment of the eag, rolf, and Shaker sequences including the S3 segment, S3-S4 loop, and S4 segment. The numbers at the top indicate the position in the eag sequence. The positions of mutations that are discussed in the text are underlined. Boxes indicate the positions of residues conserved among members of the superfamily of voltage-gated K^+ channels. Gaps have been introduced to maintain the alignment. The S3-S4 loop in Shaker is substantially longer than in eag and rolf and is shown in loops to conserve space. Overall, the sequences of eag and rolf are 23% identical. (*C*) Representative eag (*left*) and rolf (*right*) currents after expression in *Xenopus* oocytes. Eag currents were recorded in an 89 mM KCl bath solution using a two electrode voltage clamp. From a holding potential of −90 mV, currents were evoked by 150-ms pulses to test potentials from −80 to +70 mV, in 10-mV increments. Rolf currents were recorded in an excised, inside-out macropatch with 100 mM KCl in the pipette and bath solutions. The patch was held at +40 mV. Currents were evoked by perfusion of 1 mM cGMP on the cytoplasmic face of the patch.

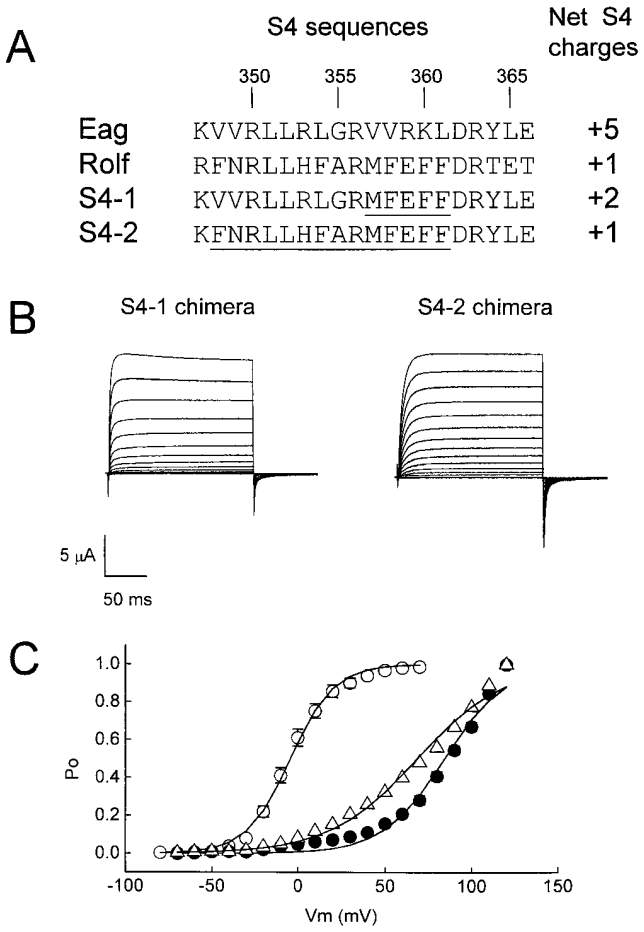

FIGURE 2. The low net charge of the S4 segment does not account for the lack of sensitivity to voltage in rolf. (*A*) The S4 sequences of eag, rolf, and the S4-1 and S4-2 chimeras. Numbers at top correspond to the position in the eag sequence. Residues that have been exchanged in the chimeras are underlined. The net charge of the S4 segment of each sequence, shown at the right, was calculated assuming R or K = +1, E or D = −1, and H = 0. (*B*) Representative current traces from the S4-1 (*left*) and S4-2 (*right*) chimeras expressed in *Xenopus* oocytes. Currents were recorded in 89 mM KCl using a two-electrode voltage clamp. From a holding potential of −90 mV, 150-ms pulses to test potentials from −30 to +120 mV were applied in 10-mV increments. (*C*) Steady-state activation curves of eag (○) and the S4-1 (●) and the S4-2 (△) chimeras. After a series of depolarizing pulses to the indicated test potentials, the amplitudes of isochronal tail currents at −90 mV were normalized to the maximum amplitude to obtain the fraction of open channels (P_o) at the test potential. Data points, shown as mean ± SEM (n = 6–8), were fit with a Boltzmann equation (*solid curves*). If error bars are not present, the SEM was smaller than the symbol shown. The activation curves of the S4-1 and S4-2 chimeras did not saturate in the tested voltage range.

TABLE I

Activation Parameters for Eag and Mutant Constructs

Construct	V_{mid}	A	V_{rest}
	mV	*mV*	*mV*
Eag	−4.3 ± 0.6(8)	12.7 ± 0.5(8)	−44.9 ± 11.1(16)
S4-1 chimera	+84.6 ± 0.7(6)	19.9 ± 0.6(6)	—
S4-2 chimera	+68.5 ± 0.6(6)	26.7 ± 0.5(6)	—
S3+loop chimera	ND	ND	−78.2 ± 8.8*(20)
Loop chimera	ND	ND	−74.2 ± 9.0*(14)
A345E	−51.9 ± 0.4(7)	14.4 ± 0.4(7)	−82.1 ± 10.9*(10)
A345R	ND	ND	−69.7 ± 6.3*(7)
L342H	+16.3 ± 0.6(4)	15.5 ± 0.5(4)	−38.3 ± 14.2(12)
Δ333-337	+11.4 ± 0.6(6)	12.8 ± 0.6(6)	−39.5 ± 5.8(15)
I317K	+3.7 ± 1.2(7)	17.6 ± 1.0(7)	−37.3 ± 7.0(10)

Values for the midpoint potential (V_{mid}) and the slope factor (A) (in mV, mean ± SEM) were derived from P_O-V curves fit with a Boltzmann equation of the form:

$$P_O(V) = 1/(1 + \exp[(V_{mid} - V)/A]),$$

where P_O is the fraction of open channels obtained from the normalized amplitude of isochronal tail currents after a depolarization to the test potential (V). Activation curves for the S4-1 and S4-2 chimeras did not saturate within the tested voltage range (see Fig. 2 *C*), leading to inaccurate values for V_{mid} and A for these mutants. Values for V_{mid} and A were not determined (ND) for the S3+loop and loop chimeras, and the A345R mutation, which shifted activation far in the hyperpolarized direction. Also shown is the resting membrane potential (V_{rest}, mean ± SD) in 1 mM KC1 for oocytes expressing each construct. V_{rest} values marked with * are significantly different from the wild-type eag control (t test, $P < 0.01$). The number of experiments, n, is given in parentheses.

S4-2 chimeras as a function of voltage (P_o-V curve) was determined by analysis of isochronal tail currents; the data were fit with a Boltzmann distribution (Fig. 2 *C*; Table I). Despite dramatic decreases in their net S4 charges, both chimeras retained significant sensitivity to voltage. It is worth noting that their P_o-V curves were less steep than that of eag, consistent with the idea that the rolf S4 segment, with its reduced net charge, contributes to the voltage sensor in the eag chimeras. In addition, the activation curves were shifted to depolarized potentials in both chimeras. The activation and deactivation kinetics of the chimeras were slightly faster than those of the wild-type eag channel (data not shown).

These data demonstrate that the low net charge of the S4 segment does not account for the voltage independence of cyclic nucleotide-gated channels such as rolf. Furthermore, the results indicate that the rolf S4 segment can support a voltage-dependent mechanism of activation in eag, albeit with reduced sensitivity to voltage. This is consistent with the idea that rolf contains a potentially functional voltage-sensing domain. As in the Shaker K^+ channel (Seoh et al., 1996), this domain may not be limited to the S4 segment.

The Relative Stability of the Open Conformation of Eag Is Significantly Increased in Chimeras Containing the S3-S4 Loop of Rolf

To investigate the mechanism by which the potentially functional voltage-sensing domain of rolf is bypassed

during its activation, other chimeras were made. We focused on the S3+loop chimera, in which the S3 segment and S3-S4 loop of eag were replaced with the corresponding region of rolf (Fig. 1 *B*). In oocytes expressing the S3+loop chimera, the resting membrane potential in 1 mM K^+ was significantly more hyperpolarized (-78 ± 9 mV, mean ± SD, $n = 20$) than in oocytes expressing wild-type eag (-45 ± 11 mV, $n = 16$) or in uninjected oocytes (-28 ± 8 mV, $n = 15$) (Table I). This suggests that the voltage-dependence of activation has been shifted to hyperpolarized potentials in the eag S3+loop chimera, so that the channel is open over a broad voltage range, stabilizing the membrane potential near the reversal potential for K^+.

To test the hypothesis that the voltage dependence of activation is shifted to hyperpolarized potentials in the S3+loop chimera, we applied a voltage ramp protocol to oocytes in 89 mM K^+. Under these conditions, the reversal potential for K^+ is close to 0 mV. From a holding potential of −10 mV, the membrane potential was ramped from −220 to +120 mV over a 500-ms interval (Fig. 3 *A*). In uninjected oocytes, only an endogenous outward current visible at potentials greater than +100 mV and small leakage and outward capacitative currents were detected. In oocytes expressing wild-type eag channels, initiating the ramp by stepping the membrane potential to −220 mV elicited a transient tail current, followed by a period of channel closure, and finally by a steeply increasing outward current detected at about 0 mV. In oocytes expressing the S3+loop chimera at levels comparable to that of eag, a prominent inward current was detected starting at ∼−200 mV, followed by a quasi-linear current-voltage relationship until ∼+100 mV, where endogenous currents were detected. The amplitude of the inward current increased between −200 and −150 mV despite a decreasing driving force for K^+, reflecting an increase in the open probability in this voltage range. These results suggest that activation of the S3+loop chimera has been shifted to very hyperpolarized potentials.

Using the ramp protocol, it was not feasible to determine accurately the potential at which activity of the S3+loop chimera can first be detected. After initiating the ramp by stepping the potential from −10 to −220 mV, the rates of channel deactivation and activation may be slow compared to the speed of the ramp, affecting the shape of the ramp-evoked current. Technical difficulties made it infeasible to surmount this problem. Slower ramps damaged the oocytes, and our voltage clamp system was not capable of sustained pulses to very hyperpolarized potentials. In addition, the S3+loop chimera did not express as robustly as the wild-type channel. In Fig. 3 *A*, the level of expression of the wild-type channel and S3+loop chimera are approximately equal. Under these circumstances, the steeply increasing outward current through eag channels was detected at ∼0 mV. However, at higher levels of eag expression, a small inward current was detected starting at ∼−40 mV, similar to the potential at which eag currents are detected in a standard current-voltage series (see Fig. 1 *C*). Therefore, if the chimera expressed at a higher level, current might be detected at a more negative potential. For these reasons, it is possible that the S3+loop chimera has a significant open probability at voltages more hyperpolarized than −200 mV.

A shift in the voltage dependence of activation to hyperpolarized potentials indicates that the relative stability of the open state of eag has been significantly increased in the S3+loop chimera. This finding suggests

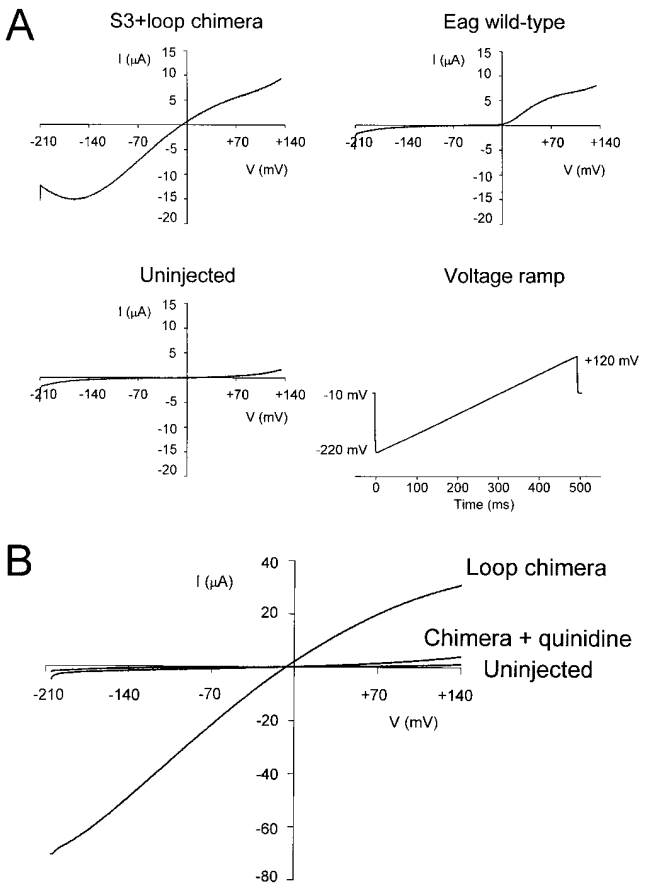

FIGURE 3. S3+loop and loop chimeras shift the activation of eag to hyperpolarized potentials. (*A*) Representative ramp-evoked currents from the S3+loop chimera, wild-type eag, and an uninjected oocyte. Currents were recorded in 89 mM KCl using a two electrode voltage clamp. From a holding potential of −10 mV, a 500-ms voltage ramp from −220 to +120 mV was applied. Large capacitive transients evoked at the beginning and end of the ramp are not shown. (*B*) Representative ramp-evoked currents from the loop chimera and an uninjected oocyte from the same batch have been superimposed. Quinidine (800 μM), which blocks eag channels, was added where indicated. Current traces were obtained as in *A*.

that rolf is voltage independent because its voltage-sensing domain is stabilized in a conformation that is permissive for channel opening. In a voltage-dependent K^+ channel, such a conformation might correspond to a state attained after the voltage-dependent conformational changes that initiate activation but precede channel opening (Zagotta and Aldrich, 1990). In eag, the rolf S3 segment and S3-S4 loop apparently shift these voltage-dependent steps to hyperpolarized voltages, thereby allowing the channel to be open over a wide range of potentials. That this phenotype can be detected implies that the partial inactivation observed in macroscopic eag currents remains incomplete even during long periods of channel activation (Robertson et al., 1996; see Fig. 1 *C*).

To narrow down the region of the S3+loop chimera that is responsible for the relative stabilization of the open state of eag, two additional chimeras were made. One, in which the S3 segment of rolf was swapped into eag, did not produce detectable currents in oocytes. The other, in which the S3-S4 loop of eag was replaced by that of rolf, was active and appeared to shift the voltage dependence of activation to very hyperpolarized potentials. Upon application of the voltage ramp protocol in 89 mM K^+, the loop chimera displayed a quasi-linear current-voltage relationship over the whole voltage range (Fig. 3 *B*). Currents resulting from expression of the loop chimera were consistently much larger than linear leak currents in uninjected oocytes from the same batch (Fig. 3 *B*). Addition of quinidine, a drug that blocks eag currents but not leak currents (Tang and Papazian, unpublished observations), reduced the amplitude of loop chimera currents to near that of leak currents measured in uninjected oocytes from the same batch (Fig. 3 *B*).

As shown in Fig. 3 *B*, transfer of the S3-S4 loop from rolf into eag is sufficient to shift the apparent voltage dependence of activation to hyperpolarized potentials. In most experiments, the chimeric channel was open at −200 mV. Occasionally, however, the amplitude of the inward current increased as the potential was ramped from −200 to −180 mV (data not shown), suggesting an increase in the open probability in this voltage range as seen in the S3+loop chimera (see Fig. 3 *A*). These results indicate that the S3-S4 loop region from rolf is primarily responsible for the increase in the relative stability of the open state of eag seen in the S3+loop chimera.

If, as has been previously reported (Brüggemann et al., 1993), eag is permeable to Ca^{2+}, the ramp-evoked currents might be contaminated by endogenous Ca^{2+}-activated Cl^- currents. However, a recent study found no evidence for Ca^{2+} permeation through eag channels (Robertson et al., 1996), a result that agrees with our own observations. We find that ionic replacement of either Ca^{2+} or Cl^- does not alter eag currents in oocytes (unpublished data).

The Mutation A345E Accounts for a Significant Portion of the Stabilization

The relative stabilization of the open state of eag in the chimeras is presumably conferred by energetic contributions from the interactions of one or more residues in the protein. To identify particular residues that contribute to the relative stabilization of the open state in the eag S3+loop and loop chimeras, we made the following mutations in eag: I317K in S3, and Δ333–337 (a deletion of the charged residues DRDED at positions 333–337), L342H, and A345E in the S3-S4 loop. In each case, the eag sequence was converted to that of rolf. These four mutations were chosen because they represent the least conservative changes between the eag and rolf sequences in the S3 segment and the S3-S4 loop; each mutation has the potential to change the charge of the eag protein (Fig. 1 *B*). All of the mutants produced functional channels (data not shown).

Of these mutations, only A345E shifted the activation of eag to hyperpolarized potentials (Fig. 4, Table I). Upon application of the ramp protocol in 89 mM K^+, inward currents were detected at ∼−90 mV (Fig. 4 *A*). Because A345E did not shift activation as far as the S3+loop or loop chimeras, it was feasible to record leak-subtracted currents in 89 mM K^+ by sustained depolarizing pulses from a holding potential of −130 mV, a voltage at which most of the channels were closed (Fig. 4 *B*). Currents were detected at −100 mV, similar to the results obtained using the ramp protocol. Analysis of isochronal tail currents revealed that the P_o-V curve for A345E was shifted by −50 mV compared to that of wild-type eag (Fig. 4 *C*, Table I). These results indicate that the A345E mutation contributes significantly to the shift in activation seen in the S3+loop and loop chimeras, but is not solely responsible for it. The A345E mutation did not change the steepness of the activation curve (Fig. 4 *C*, Table I), indicating that the mutation affects the relative stability of open and closed conformations without altering the voltage-dependence of eag.

Other Charge-changing Mutations in S3 and the S3-S4 Loop Do Not Contribute to the Stabilization

The P_o-V curves of the mutants I317K, Δ333–337, and L342H were determined by analysis of isochronal tail currents. Unlike A345E, these charge-changing mutations did not shift the activation of eag to hyperpolarized potentials (Fig. 5, Table I). Rather, their activation curves were shifted in the depolarized direction.

One significant difference between the eag and rolf sequences in the S3-S4 loop is the presence of the

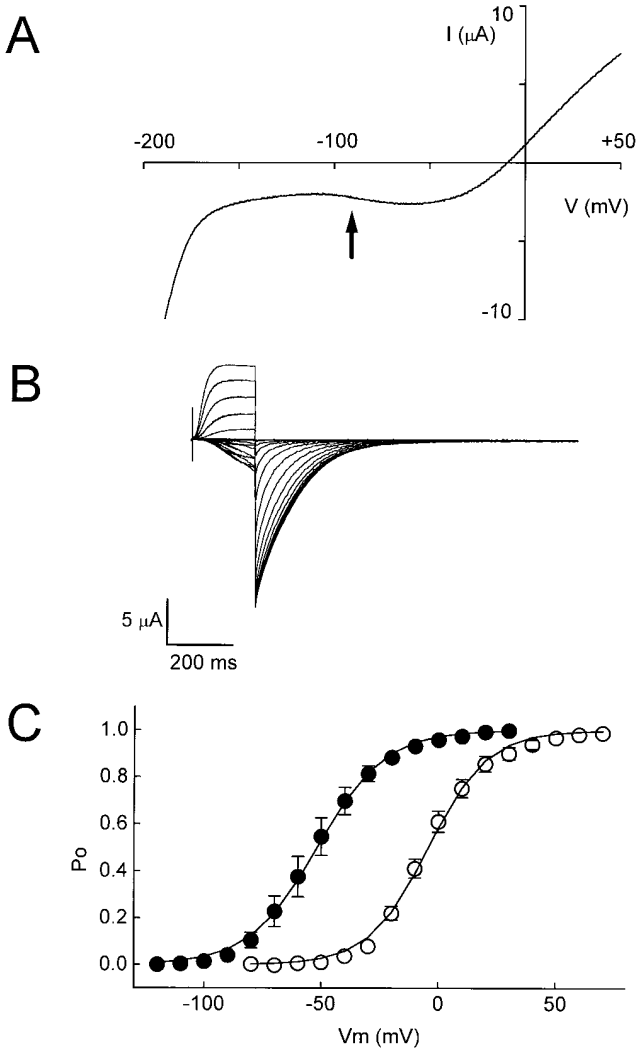

FIGURE 4. The mutation A345E in the S3-S4 loop of eag shifts activation in the hyperpolarized direction. (*A*) Representative current was evoked by a 500-ms voltage ramp from −220 to +60 mV. The arrow indicates that inward current is first detected at about −90 mV. (*B*) Representative, leak-subtracted current traces from A345E expressed in oocytes. Currents were recorded in 89 mM KCl using a two-electrode voltage clamp. From a holding potential of −130 mV, 200-ms pulses to potentials ranging from −120 to +30 mV were applied in 10-mV increments. Leakage currents were subtracted using the P/−4 protocol (Bezanilla and Armstrong, 1977). (*C*) Steady-state activation curves of eag (○) and A345E (●). After a series of depolarizing pulses to the indicated test potentials, the amplitudes of isochronal tail currents at −90 mV (eag) or −130 mV (A345E) were normalized to the maximum amplitude to obtain the P_o at the test potential. Data points, shown as mean ± SEM (n = 7–8), were fit with a Boltzmann equation (*solid curves*). If error bars are not present, the SEM was smaller than the symbol shown.

charged amino acids DRDED at positions 333–337 in eag (Fig. 1 *B*). In the Δ333–337 mutant, activation was shifted ~15 mV in the depolarized direction. Although small, this shift is in the correct direction to be caused

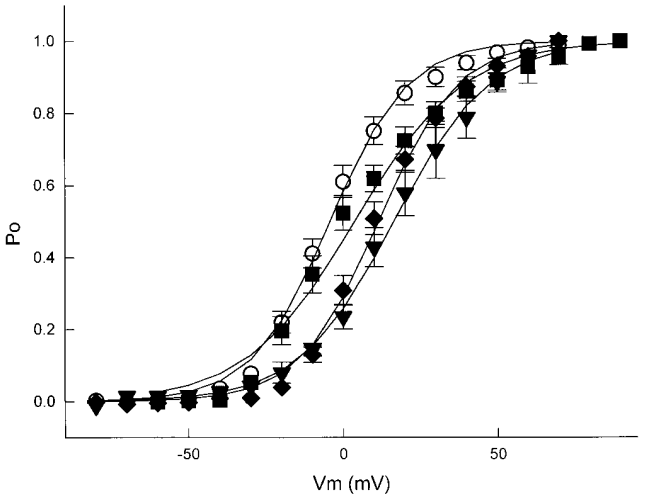

FIGURE 5. Mutations I317K, D333-337, and L342H do not shift the activation of eag in the hyperpolarized direction. The P_o-V curves of eag (○), I317K (■), Δ333–337 (◆), and L342H (▼) were obtained from the analysis of isochronal tail currents recorded at −90 mV, as in Figs. 2 and 4.

by a field effect on the voltage sensor in eag. In addition, the rate of activation was two to three times slower than in wild-type eag (data not shown).

In rolf, the S3-S4 loop is six amino acids shorter than in eag, and much shorter than in Shaker (Fig. 1 *B*). This raises the possibility that the shorter loop in rolf contributes to the channel's insensitivity to voltage, perhaps by constraining the conformational flexibility of the S4 segment. According to our analysis of Δ333–337, this explanation is unlikely. In Δ333–337, the loop is only one residue longer than in rolf, yet the channel is voltage dependent. The Δ333–337 mutation slows the kinetics of activation, however.

Either Positively or Negatively Charged Residues at Position 345 in Eag Increase the Relative Stability of the Open Conformation

Of the four charge-changing mutations that have been studied, only A345E shifts the activation of eag in the hyperpolarized direction. Several mechanisms could account for the increased relative stability of the open state in A345E, including: (*a*) a surface-potential effect exerted by the negatively charged glutamate, (*b*) an electrostatic interaction between the introduced glutamate and another residue in the protein, and (*c*) a change in conformational stability induced by the polar or charged nature of the glutamate. The first two mechanisms depend on the negative charge of the glutamate residue. Substituting A345 by a positively charged residue would be expected to have a qualita-

tively different effect than the A345E mutation. In contrast, if the third mechanism applies, the mutation A345R would be expected to have a qualitatively similar effect to A345E.

The eag mutation A345R was made and expressed in *Xenopus* oocytes. Upon application of a voltage ramp from −220 to +60 mV in 89 mM K^+, it was apparent that the A345R mutation shifted the activation of eag to hyperpolarized potentials, similarly to A345E (Fig. 6 *A*). In A345R, the ramp-evoked current was detected at a more hyperpolarized potential than in A345E, suggesting that A345R increases the relative stability of the open state somewhat more than A345E. Inward currents evoked by sustained pulses from a holding potential of −150 mV were detected at ∼−130 mV (Fig. 6 *B*).

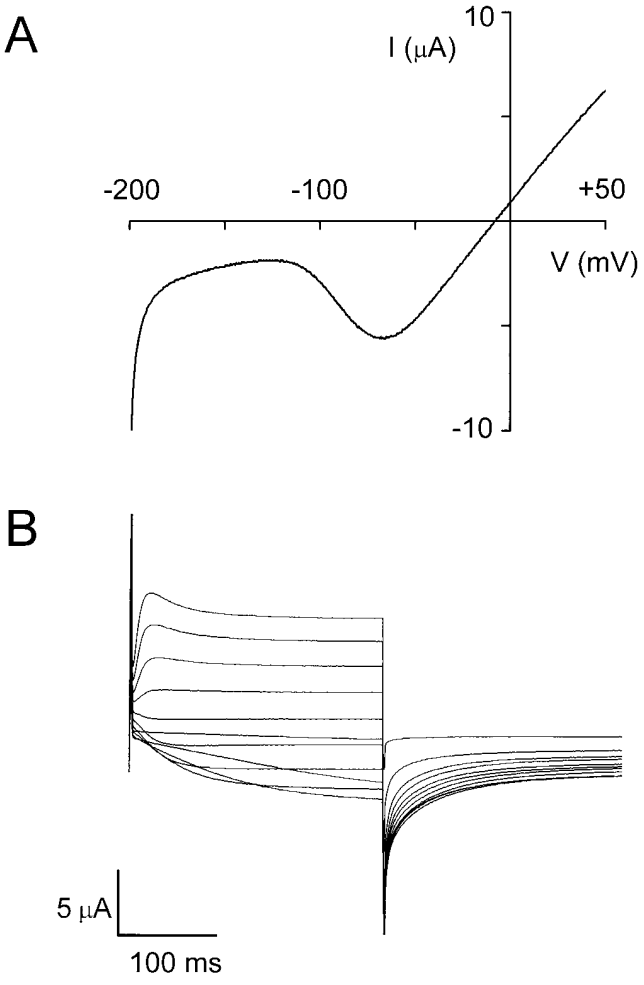

FIGURE 6. The mutation A345R in the S3-S4 loop of eag shifts activation in the hyperpolarized direction. (*A*) Representative current was evoked by a voltage ramp as in Fig. 4. (*B*) Representative current traces from A345R expressed in oocytes. Currents were recorded in 89 mM KCl using a two electrode voltage clamp. From a holding potential of −150 mV, 250-ms pulses to potentials ranging from −130 to +70 mV were applied in 20-mV increments. The current reversed at about −5 mV. Leakage currents were not subtracted.

These results are consistent with the idea that A345E and A345R increase the relative stability of the open state by a mechanism that depends on the hydrophilic or charged nature of the substitution rather than on the particular charge of the residue. One possibility is that position 345 may be exposed to the aqueous environment in the open state, but not in closed states. Compared to the original alanine, conversion to either glutamate or arginine would increase the relative stability of the open state, in which the residue is exposed to solvent. In rolf, the glutamate at the analogous position may be exposed. Difficulty in burying this residue in a hydrophobic environment may be one of several structural factors that contribute to stabilizing the potentially functional voltage-sensing domain in a conformation that is permissive for pore opening.

DISCUSSION

Transfer of Voltage Independence from Rolf to Eag

Cyclic nucleotide-gated channels have little or no inherent sensitivity to voltage (Haynes and Yau, 1990; Goulding et al., 1992). They are, however, members of the superfamily of voltage-gated ion channels and contain conserved charged residues that contribute to the voltage sensors of Na^+ and K^+ channels (Jan and Jan, 1990). To determine what accounts for the lack of voltage sensitivity in a cyclic nucleotide-gated channel from the rat olfactory system (rolf), we made chimeras between rolf and ether-à-go-go (eag), a voltage-dependent K^+ channel from *Drosophila*. Because the S4 segment has been demonstrated to be a major component of the voltage sensor in Na^+ and K^+ channels (Aggarwal and MacKinnon, 1996; Larsson et al., 1996; Seoh et al., 1996; Yang et al., 1996), we tested the hypothesis that rolf is insensitive to voltage because its S4 segment has a reduced net charge. Two chimeras, in which portions of the rolf S4 segment were transferred into eag, were voltage dependent. Therefore, the low net S4 charge in rolf cannot account for its lack of sensitivity to voltage. In fact, the S4 segment of rolf can support a voltage-dependent mechanism of activation in eag. These results are consistent with the idea that cyclic nucleotide-gated channels such as rolf contain a potentially functional voltage-sensing domain that is normally silent during gating.

The S3-S4 loop is shorter in rolf than in many voltage-dependent K^+ channels, including eag and Shaker (Tempel et al., 1987; Dhallan et al., 1990; Warmke et al., 1991; Chandy and Gutman, 1994; Warmke and Ganetzky, 1994), raising the possibility that the short loop constrains the movement of the S4 segment in

rolf. Our results argue against this mechanism because a deletion mutation in eag, Δ333–337, has a loop similar in length to that of rolf, but causes no decrease in voltage sensitivity.

Alternatively, the putative voltage-sensing domain could be bypassed during activation if it were stabilized in an activated conformation that is permissive for pore opening. Evidence for this mechanism was obtained by analysis of the S3+loop and loop chimeras. Both shifted the activation of eag to very hyperpolarized potentials. We conclude that these chimeric channels are voltage-independent in the physiological range of membrane potentials. Upon expression in *Xenopus* oocytes, rolf displays a similar behavior. Fig. 7 shows the rolf current evoked by a voltage ramp from −120 to +120 mV in an excised, inside-out macropatch. The bath and pipette solutions contained 100 mM K^+. To open the channel, 1 mM cGMP was applied to the cytoplasmic face of the patch. Rolf displayed a quasi-linear current-voltage relationship very similar to that seen in the eag S3+loop and loop chimeras over the same voltage range (Fig. 7). Although it would be advantageous to analyze the behavior of the eag chimeras in excised, inside-out patches, such experiments have not been feasible because eag rapidly runs down in cell-free patches (Robertson et al., 1996).

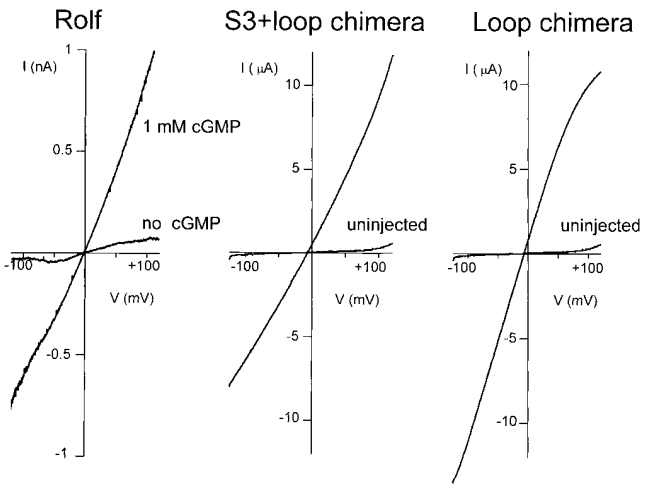

FIGURE 7. Rolf, and the S3+loop and loop chimeras display similar quasi-linear current-voltage relationships in the physiological range of membrane potentials. Representative currents were evoked by a 500-ms voltage ramp from −120 to +120 mV. The holding potential was 0 mV for rolf and −10 mV for the two chimeras. Rolf currents were recorded in an excised, inside-out macropatch in the presence or absence of 1 mM cGMP (*left*). Ramp-evoked currents from the S3+loop (*middle*) and loop (*right*) chimeras were recorded using a two-electrode voltage clamp; also shown are ramp-evoked currents from uninjected oocytes.

Our results suggest that rolf is independent of membrane potential in the physiological range because its voltage-sensing domain is stabilized in a conformation permissive for channel opening. This conformation may be similar to that attained in a voltage-gated channel after the voltage-dependent transitions that accompany activation. In channels such as Shaker, voltage-dependent conformational changes prime the channel for pore opening, which is a less voltage-dependent transition that may be cooperative (Sigworth, 1993; Bezanilla et al., 1994; Zagotta et al., 1994). In cyclic nucleotide-gated channels such as rolf, the channel is already primed for pore opening, which occurs via an allosteric mechanism (Goulding et al., 1994). Binding of the cyclic nucleotide ligand stabilizes the open conformation (Goulding et al., 1994).

Although our results are suggestive, it is important to note that we cannot conclude that the S3-S4 loop is solely responsible for the lack of voltage dependence in rolf. If the rolf channel is indeed stabilized in a conformation permissive for pore opening, both the S3-S4 loop and additional structural features are likely to contribute. Our data do suggest, however, that the structural and functional homology of distantly related members of the superfamily of voltage-gated channels may not be limited to the pore region (Heginbotham et al., 1992; Goulding et al., 1993), but might also include the S2, S3, and S4 transmembrane segments that contribute to a voltage-sensing domain in voltage-gated channels such as Shaker (Papazian et al., 1995; Seoh et al., 1996; Tiwari-Woodruff et al., 1997). In voltage-dependent channels, the conformation of the voltage-sensing domain is readily influenced by the membrane potential. In voltage-insensitive channels, the conformational flexibility of this domain may be much reduced due to a significant increase in the relative stability of the activated conformation.

Stabilization of the Open State of Eag

The S3+loop and loop chimeras shift the activation of eag to hyperpolarized potentials, although technical limitations made it difficult to determine the actual magnitude of the shift. The shape of ramp-evoked currents depends on the speed of the ramp compared to the rates of channel deactivation and activation. In particular, slowly deactivating channels could contribute to the ramp-evoked currents at hyperpolarized potentials. However, the bulk of our evidence, especially the data obtained from A345E and A354R using sustained voltage steps, make it extremely unlikely that this explanation can fully account for our results.

The S3+loop and loop chimeras provide an opportunity to identify some of the residues and structural interactions that stabilize the open conformation of a voltage-dependent K^+ channel. Because large shifts in the voltage range of activation may correspond to fairly small changes (several kcal/mol) in the relative free

energy difference between conformational states (Sigworth, 1993), the shift in the activation of eag could be achieved by small alterations in the structure. Our results indicate that much of the stabilization is imparted to eag by the S3-S4 loop of rolf, although we cannot rule out some contribution by residues in the S3 segment. The mutation A345E accounts for a significant part of the shift. Therefore, the increase in the relative stability of the open state of eag in the S3+loop and loop chimeras is probably due to free energy contributions from a limited number of residues or structural interactions.

The oppositely charged substitutions A345E and A345R had qualitatively similar effects on the activation of eag. Therefore, the stabilization of the open state does not depend on the charge of the residue, ruling out field effects or electrostatic interactions as the underlying mechanism. An alternative possibility is that position 345 is buried in closed channels and exposed to solvent in the activated conformation. Compared to alanine, both glutamate and arginine would prefer an aqueous environment to a hydrophobic one.

The proposal that position 345 is exposed to solvent in open channels is consistent with a recent report from Mannuzzu et al. (1996). Cysteine residues were introduced into the S3-S4 loop of Shaker channels and labeled with a sulfhydryl-reactive fluorescent probe. Upon voltage-dependent activation of the channel, the fluorescence of the probe at some loop positions was decreased, an effect which was attributed to increased solvent exposure concurrent with gating.

Our results indicate that position 345 is not solely responsible for the shift in activation seen in the loop chimera. There may be other eag-to-rolf point mutations in this region which, when combined with A345E, will recapitulate the shifts seen in the chimeric channels. In Shaker channels, combination of three S4 mutations caused a much larger shift of activation to hyperpolarized potentials than was observed in each mutant individually (Miller and Aldrich, 1996).

Lack of Correspondence between Net S4 Charge and Voltage Sensitivity

In voltage-gated K^+ channels, the positively charged S4 residues do not contribute equally to the voltage sensor (Papazian et al., 1991; Aggarwal and MacKinnon, 1996; Seoh et al., 1996). Consistent with this finding, our results demonstrate that the net charge of the S4 segment is not sufficient to determine the voltage sensitivity of eag. This conclusion contrasts with a previous report, in which the S4 segments of two voltage-gated K^+ channels, RCK1 (rKv1.1) and Shab 11 (dKv2.1) were exchanged (Logothetis et al., 1993). In the resulting chimeras, the position and steepness of steady-state activation curves corresponded to those of the S4 donor, which is clearly not the case in our study. This suggests that one or more residues outside the S4 segment make significant contributions to the voltage sensor of eag, as in Shaker K^+ channels (Seoh et al., 1996).

To conclude, our results suggest that the functional and structural homology of distantly related members of the superfamily of voltage-gated channels includes the voltage-sensing domain. Further analysis of cyclic nucleotide-gated channels and the voltage-insensitive eag loop chimera promises to provide insights into the activated conformation of voltage-gated ion channels.

We are grateful to Drs. Gail Robertson and Randall Reed for the eag and rolf clones, and to Dr. Emily Liman for the vector pGEMHE. We thank Dr. Francisco Bezanilla for helpful discussions; Dr. Sally Krasne, Dr. Enrico Stefani, and members of the Papazian lab for comments on the manuscript; and the Department of Physiology and the laboratories of Drs. Ernest M. Wright and H. Ronald Kaback for their help and support.

This work was supported by grants from the Keck Foundation, the Pew Charitable Trusts, and the National Institutes of Health (GM43459).

Original version received 30 September 1996 and accepted version received 15 November 1996.

REFERENCES

Aggarwal, S.K., and R. MacKinnon. 1996. Contribution of the S4 segment to the gating charge in the Shaker K^+ channel. *Neuron.* 16:1169–1177.

Altenhofen, W., J. Ludwig, E. Eismann, W. Kraus, W. Bönigk, and U.B. Kaupp. 1991. Control of ligand specificity in cyclic nucleotide-gated channels from rod photoreceptors and olfactory epithelium. *Proc. Natl. Acad. Sci. USA.* 88:9868–9872.

Bezanilla, F., and C.M. Armstrong. 1977. Inactivation of the sodium channel. I. Sodium current experiments. *J. Gen. Physiol.* 70:549–566.

Bezanilla, F., E. Perozo, and E. Stefani. 1994. Gating of Shaker K^+ channels. II. The components of gating currents and a model of channel activation. *Biophys. J.* 66: 1011–1021.

Brüggemann, A., L.A. Pardo, W. Stühmer, and O. Pongs. 1993. Ether-à-go-go encodes a voltage-gated channel permeable to K^+ and Ca^{2+} and modulated by cAMP. *Nature (Lond.).* 365:445–448.

Chandy, K.G., and G.A. Gutman. 1994. Voltage-gated potassium channel genes. *In* Ligand- and Voltage-Gated Ion Channels, R.A. North, editor. CRC Press, Boca Raton, FL. 1–71.

Dhallan, R.S., K.-W. Yau, K.A. Schrader, and R.R. Reed. 1990. Primary structure and functional expression of a cyclic nucleotide-activated channel from olfactory neurons. *Nature (Lond.).* 347: 184–187.

Gordon, S.E., and W.N. Zagotta. 1995. Localization of regions affecting an allosteric transition in cyclic nucleotide-activated channels. *Neuron.* 14:857–864.

Goulding, E.H., J. Ngai, R.H. Kramer, S. Colicos, R. Axel, S.A Siegelbaum, and A. Chess. 1992. Molecular cloning and single-channel properties of the cyclic nucleotide-gated channel from catfish olfactory neurons. *Neuron.* 8:45–58.

Goulding, E.H., G.R. Tibbs, D. Liu, and S.A. Siegelbaum. 1993. Role of H5 domain in determining pore diameter and ion permeation through cyclic nucleotide-gated channels. *Nature (Lond.).* 364:61–64.

Goulding, E.H., G.R. Tibbs, and S.A. Siegelbaum. 1994. Molecular mechanism of cyclic nucleotide-gated channel activation. *Nature (Lond.).* 372:369–374.

Guy, H.R., S.R. Durell, J. Warmke, R. Drysdale, and B. Ganetzky. 1991. Similarities in amino acid sequences of *Drosophila* eag and cyclic nucleotide-gated channels. *Science (Wash. DC).* 254:730.

Haynes, L.W., and K.-W. Yau. 1990. Single channel measurement from the cyclic GMP-activated conductance of catfish retinal cones. *J. Physiol. (Lond.).* 429:451–481.

Heginbotham, L., T. Abramson, and R. MacKinnon. 1992. A functional connection between the pores of distantly-related ion channels as revealed by mutant K^+ channels. *Science (Wash. DC).* 258:1152–1155.

Hodgkin, A.L., and A.F. Huxley. 1952. A quantitative description of membrane current and its application to conduction and excitation in nerve. *J. Physiol. (Lond.).* 117:500–544.

Horton, R.M., H.D. Hunt, S.N. Ho, J.K. Pullen, and L.R. Pease. 1989. Engineering hybrid genes without the use of restriction enzymes: gene splicing by overlapping extension. *Gene.* 77:61–68.

Jan, L.Y., and Y.N. Jan. 1990. A superfamily of ion channels. *Nature (Lond.).* 345:672.

Jan, L.Y., and Y.N. Jan. 1992. Tracing the roots of ion channels. *Cell.* 69:715–718.

Kaupp, U.B., T. Niidome, T. Tanabe, S. Terada, W. Bönigk, W. Stühmer, N.J. Cook, K. Kangawa, H. Matsuo, T. Hirose, et al. 1989. Primary structure and functional expression from complementary DNA of the rod photoreceptor cyclic GMP-gated channel. *Nature (Lond.).* 342:762–766.

Larsson, H.P., O.S. Baker, D.S. Dhillon, and E.Y. Isacoff. 1996. Transmembrane movement of the Shaker K^+ channel S4. *Neuron.* 16:387–397.

Liman, E.R., P. Hess, F. Weaver, and G. Koren. 1991. Voltage-sensing residues in the S4 region of a mammalian K^+ channel. *Nature (Lond.).* 353:752–756.

Liman, E.R., J. Tytgat, and P. Hess. 1992. Subunit stoichiometry of a mammalian K^+ channel determined by construction of multimeric cDNAs. *Neuron.* 9:861–871.

Logothetis, D.E., B.F. Kammen, K. Lindpaintner, D. Bisbas, and B. Nadal-Ginard. 1993. Gating charge differences between two voltage-gated K^+ channels are due to the specific charge content of their respective S4 regions. *Neuron.* 10:1121–1129.

Logothetis, D.E., S. Movahedi, C. Satler, K. Lindpaintner, and B. Nadal-Ginard. 1992. Incremental reductions of positive charge within the S4 region of a voltage-gated K^+ channel result in corresponding decreases in gating charge. *Neuron.* 8:531–540.

Mannuzzu, L.M., M.M. Moronne, and E.Y. Isacoff. 1996. Direct physical measure of conformational rearrangement underlying potassium channel gating. *Science (Wash. DC).* 271:213–216.

Miller, A.G., and R.W. Aldrich. 1996. Conversion of a delayed rectifier K^+ channel to a voltage-gated inward rectifier K^+ channel by three amino acid substitutions. *Neuron.* 16:853–858.

Miller, C. 1991. 1990: annus mirabilis of potassium channels. *Science (Wash. DC).* 252:1092–1096.

Papazian, D.M., X.M. Shao, S.-A. Seoh, A.F. Mock, Y. Huang, and D.H. Wainstock 1995. Electrostatic interactions of S4 voltage sensor in Shaker K^+ channel. *Neuron.* 14:1293–1301.

Papazian, D.M., L.C. Timpe, Y.N. Jan, and L.Y. Jan. 1991. Alteration of voltage-dependence of Shaker potassium channel by mutations in the S4 sequence. *Nature (Lond.).* 349:305–310.

Perozo, E., L. Santacruz-Toloza, E. Stefani, F. Bezanilla, and D.M. Papazian. 1994. S4 mutations alter gating currents of Shaker K^+ channels. *Biophys. J.* 66:345–354.

Planells-Cases, R., A.V. Ferrer-Montiel, C.D. Patten, and M. Montal. 1995. Mutation of conserved negatively charged residues in the S2 and S3 transmembrane segments of a mammalian K^+ channel selectively modulates channel gating. *Proc. Natl. Acad. Sci. USA.* 92:9422–9426.

Robertson, G.A., J.W. Warmke, and B. Ganetzky. 1996. Potassium currents expressed from *Drosophila* and mouse *eag* cDNAs in *Xenopus* oocytes. *Neuropharmacology.* 35:841–850.

Seoh, S.-A., D. Sigg, D.M. Papazian, and F. Bezanilla. 1996. Voltage-sensing residues in the S2 and S4 segments of the Shaker K^+ channel. *Neuron.* 16:1159–1167.

Sigworth, F.J. 1993. Voltage-gating of ion channels. *Q. Rev. Biophys.* 27:1–40.

Strong, M., K.G. Chandy, and G.A. Gutman. 1993. Molecular evolution of voltage-sensitive ion channel genes: on the origins of electrical excitability. *Mol. Biol. Evol.* 10:221–242.

Stühmer, W., F. Conti, H. Suzuki, X. Wang, M. Noda, N. Yahagi, H. Kubo, and S. Numa. 1989. Structural parts involved in activation and inactivation of the sodium channel. *Nature (Lond.).* 339:597–603.

Tempel, B.L., D.M. Papazian, T.L. Schwarz, Y.N. Jan, and L.Y. Jan. 1987. Sequence of a probable potassium channel component encoded at Shaker locus of *Drosophila. Science (Wash. DC).* 237:770–775.

Timpe, L.C., T.L. Schwarz, B.L. Tempel, D.M. Papazian, Y.N. Jan, and L.Y. Jan. 1988. Expression of functional potassium channels from Shaker cDNA in *Xenopus* oocytes. *Nature (Lond.).* 331:143–145.

Tiwari-Woodruff, S.K., C.T. Schulteis, A.F. Mock, and D.M. Papazian. 1997. Electrostatic interactions between transmembrane segments mediate folding of Shaker K^+ channel subunits. *Biophys. J.* In press.

Varnum, M.D., K.D. Black, and W.N. Zagotta. 1995. Molecular mechanism for ligand discrimination of cyclic nucleotide-gated channels. *Neuron.* 15:619–625.

Warmke, J., R. Drysdale, and B. Ganetzky. 1991. A distinct potassium channel polypeptide encoded by the *Drosophila* eag locus. *Science (Wash. DC).* 252:1560–1562.

Warmke, J.W., and B. Ganetzky. 1994. A family of potassium channel genes related to eag in *Drosophila* and mammals. *Proc. Natl. Acad. Sci. USA.* 91:3438–3442.

Weiss, J.N., N. Venkatesh, and S.T. Lamp. 1992. ATP-sensitive K^+ channels and cellular K^+ loss in hypoxic and ischaemic mammalian ventricle. *J. Physiol. (Lond.).* 447:649–673.

Yang, N., A.L. George, and R. Horn. 1996. Molecular basis of charge movement in voltage-gated sodium channels. *Neuron.* 16: 113–122.

Yang, N., and R. Horn. 1995. Evidence for voltage-dependent S4 movement in sodium channels. *Neuron.* 15:213–218.

Zagotta, W.N., and R.W. Aldrich. 1990. Voltage-dependent gating of Shaker A-type potassium channels in *Drosophila* muscle. *J. Gen. Physiol.* 95:29–60.

Zagotta, W.N., T. Hoshi, and R.W. Aldrich. 1994. Shaker potassium channel gating III: evaluation of kinetic models for activation. *J. Gen. Physiol.* 103:321–362.